

Photorefraction of Pb-doped tin hypthiodiphosphate

A. Shumelyuk^{a,*}, D. Barilov^a, M. Imlau^b, A. Grabar^c, I. Stoyka^c, Yu. Vysochanskii^c

^a *Institute of Physics, National Academy of Sciences, 03650, Kiev-39, Ukraine*

^b *Fachbereich Physik, University of Osnabrück, D-49076 Osnabrück, Germany*

^c *Institute of Solid State Physics and Chemistry, University of Uzhgorod, 88 000 Uzhgorod, Ukraine*

Received 15 July 2007; received in revised form 21 September 2007; accepted 1 October 2007

Available online 19 November 2007

Abstract

Photorefractive properties of deliberately lead-doped tin hypthiodiphosphate ($\text{Sn}_2\text{P}_2\text{S}_6$, SPS) are investigated. In contrast to nominally undoped crystals, the space-charge gratings are formed by charge species of only one type, holes, what ensures a high beam-coupling gain in the steady-state. No optical sensitization is needed for the recording with near infrared light, but a photorefractive sensitivity does not extend beyond a wavelength of $0.9 \mu\text{m}$. Like for some other SPS crystals, in SPS:Pb the effective trap density was found to be intensity dependent in the red spectral range.

© 2007 Published by Elsevier B.V.

PACS: 42.65.Hw; 42.70.Nq

Keywords: Photorefraction of ferroelectrics; Charge transport and redistribution; Electrooptic effect

1. Introduction

Tin hypthiodiphosphate ($\text{Sn}_2\text{P}_2\text{S}_6$, SPS) is known as a promising photorefractive material for the recording in the red and near infrared spectral range with high gain factor and rather short decay time (see, e.g., the review articles [1,2]). The largest amount of information is gathered so far for nominally undoped SPS crystals [2,3]. It has been shown that pre-exposure of the crystal to visible light with a quantum energy close to the forbidden band gap results in a considerable enhancement of the two-beam coupling gain factor at $\lambda = 1.06 \mu\text{m}$ [3]. This was interpreted as a light-induced change of the effective trap density from $N_{\text{eff}} \approx 7.3 \times 10^{14} \text{ cm}^{-3}$ for a virgin crystal to $N_{\text{eff}} \approx 7.7 \times 10^{15} \text{ cm}^{-3}$ after pre-exposure [3]. Further, the effect of grating self enhancement was discovered when recording with He–Ne laser light with probably the same origin: Light

with larger intensity ensured a larger gain factor [4]. The ultimate effective trap density measured in red light experiments was $N_{\text{eff}} \approx 10^{16} \text{ cm}^{-3}$.

These data allow to claim that the photorefractive efficiency of SPS can be considerably improved by technological means, e.g., via controlling the type and density of traps with appropriate impurities added during the growth procedure. Successful attempts in this direction have already been reported with Te and Sb-doped SPS crystals [5] and so called “modified” brown SPS crystals [6], especially in the near-infrared spectral range. The present paper describes the results of a photorefractive characterization of Pb-doped SPS crystals in the spectral range accessible with a Kr^+ -laser and a Ti:Sapphire-laser. It is shown that this material ensures the steady-state two-beam coupling gain factor nearly as large as the steady-state gain factor determined for nominally undoped crystals, i.e., no compensating grating is revealed. A relatively high steady-state gain factor manifests itself in Pb-doped SPS with no preliminary exposure to white light, i.e., no sensitizing procedure is necessary as compared with nominally undoped crystals.

* Corresponding author. Tel.: +380 44 525 08 18; fax: +380 44 525 23 59.

E-mail address: shumeluk@iop.kiev.ua (A. Shumelyuk).

2. Experimental procedure

The SPS crystals are grown by standard vapour-transport technique. Lead is loaded in the tube in the pure state with a concentration of about 1 wt.%. The SPS:Pb sample is cut along the crystallographic axes with dimensions $x \times y \times z = 5 \times 7 \times 3 \text{ mm}^3$. Faces normal to the z -axis are optically finished. The results obtained are compared to that known for standard nominally undoped crystals (“yellow SPS” [1] or type-I SPS [4,7]).

The transmission-type dynamic gratings are recorded with cw-radiation of a TEM₀₀ Kr⁺-laser of wavelengths $\lambda = 0.568 \text{ }\mu\text{m}$ (120 mW output power), $\lambda = 0.647 \text{ }\mu\text{m}$ (400 mW), and TEM₀₀ Ti:Sapphire-laser $\lambda = (0.75\text{--}0.9) \text{ }\mu\text{m}$ (700 mW). These two lasers, as it will be seen from what follows, cover nearly the whole range of photorefractive sensitivity of Pb-doped tin Hypothiodiphosphate. The unexpanded laser beam is used in all experiments. The light is polarized in the plane of beam intersection. The samples are aligned so that the photorefractive grating vector is parallel to the x -axis to profit from the presumably largest known (for undoped SPS) electrooptic coefficient $r_{111} = 174 \text{ pm/V}$ [8].

The dynamics of the two-beam coupling is studied in the transmission grating geometry. The measured quantities are the two-beam coupling gain [9]

$$\Gamma = \frac{1}{\ell} \ln \frac{I_s}{I_s(0)}, \quad (1)$$

with the interaction length ℓ and the intensity of the (weak) output signal wave I_s in the presence of the strong pump beam with the intensity $I_p \gg I_s$ and $I_s(0)$ without the pump wave and the characteristic exponential build-up (or decay) time of the refractive index grating τ . These quantities have been measured at various experimental parameters (grating spacing Λ , total light intensity I_0 , intensity ratio I_s/I_p , light wavelength λ). From the experimental dependences we extract the Debye screening length that allows for evaluating the effective trap density, the diffusion length and therefore to estimate the lifetime-mobility product, the photo and dark conductivities, and the effective electrooptic constant that accounts for the degree of the poling. These data are compared to those known for nominally undoped material.

3. Experimental results and discussion

The temporal dynamics of the weak beam amplification which is due to beam coupling is shown in Fig. 1 for (a) SPS:Pb and (b) nominally undoped SPS of type I, respectively [4,7]. The dependences are quite different: As distinct for nominally undoped SPS [3], for lead-doped material the initially achieved high gain does not drop down with time. This points to a much smaller amplitude and much longer build-up time of the out-of-phase secondary grating [10] in SPS:Pb, if any grating of this kind exists at all. Qualitatively similar results have been obtained at all wavelengths from $0.568 \text{ }\mu\text{m}$ till $0.9 \text{ }\mu\text{m}$. No beam coupling and no grat-

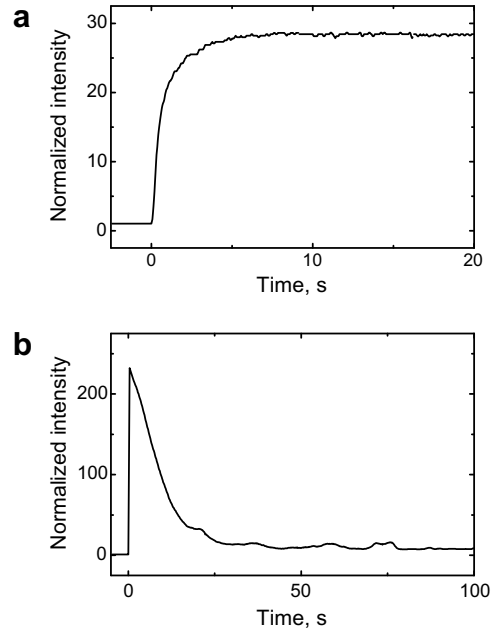


Fig. 1. Temporal evolution of the signal wave amplified because of two-beam coupling, (a) for SPS:Pb and (b) for nominally undoped type-I SPS. Pump-signal intensity ratio is 1000:1, total light intensity in the sample 1 W/cm^2 , $\Lambda \approx 1.9 \text{ }\mu\text{m}$, $\lambda = 647 \text{ nm}$.

ing recording was observed in SPS:Pb at $\lambda = 1.06 \text{ }\mu\text{m}$. From the direction of the intensity transfer we conclude that within the whole range of photorefractive sensitivity the movable charge carriers in SPS:Pb are holes, similar to nominally undoped SPS [11].

The grating spacing dependences of the gain factor $\Gamma = \Gamma(\Lambda)$ are shown in Fig. 2 for different recording wavelengths. When measuring these dependences we kept a high intensity of the recording light $> 2 \text{ W/cm}^2$. The solid lines show best fits of the dependences calculated for crystals under the assumptions of one type of movable charge carriers [9]

$$\Gamma = \frac{4\pi^2 n^3 r_{\text{eff}} k_B T}{\lambda \Lambda e \cos \theta} \cdot \frac{1}{1 + (\kappa I / \sigma_d)} \cdot \frac{1}{1 + K^2 \ell_s^2}, \quad (2)$$

to the experimental data. Here r_{eff} is the effective electrooptic coefficient, n is the refractive index, k_B is Boltzmann's

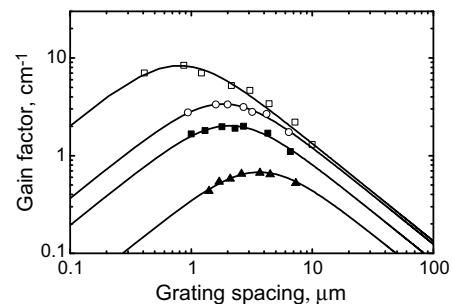


Fig. 2. Dependences of two-beam coupling gain factor Γ on grating spacing Λ for $\lambda = 0.568 \text{ }\mu\text{m}$ (open squares), $0.800 \text{ }\mu\text{m}$ (open dots), $0.850 \text{ }\mu\text{m}$ (filled dots), and $0.875 \text{ }\mu\text{m}$ (filled triangles).

constant, T is the absolute temperature, e is the electron charge, θ is the half-angle between the recording beams inside the sample, σ_d is the dark conductivity, κ is the specific photoconductivity, $K = 2\pi/\Lambda$ is the grating spatial frequency and ℓ_s is the Debye screening length:

$$\ell_s = \sqrt{\frac{\epsilon\epsilon_0 k_B T}{e^2 N_{\text{eff}}}}. \quad (3)$$

Two crystal parameters can be extracted from the fitting procedure, the effective electrooptic coefficient r_{eff} and the Debye screening length ℓ_s . The value of electrooptic coefficient strongly depends on quality of sample poling (i.e. on amount of residual 180° domains that remain in the sample after poling procedure). The screening length is, fortunately, insensitive to quality of poling and allows to evaluate the effective trap density if the dielectric constant of the crystal is known. Only ℓ_s (and N_{eff}) are evaluated from fitting the experimental data of Fig. 2.

Each of these dependences has a pronounced maximum at grating spacing $\Lambda = 2\pi\ell_s$. This allows to evaluate the effective trap density N_{eff} if the dielectric constant of SPS is known [1].

Fig. 3a shows the photon energy dependences of the Debye screening length ℓ_s , extracted from the data similar to shown in Fig. 2. It can be seen that the screening length is increasing by roughly two times within the wavelength range from 568 nm to 885 nm and drastically increases beyond 875 nm. The photon energy dependence of N_{eff} is shown in Fig. 3b. It should be underlined that the screening length becomes smaller than $1 \mu\text{m}$ near the bandedge. This was never observed for nominally undoped material.

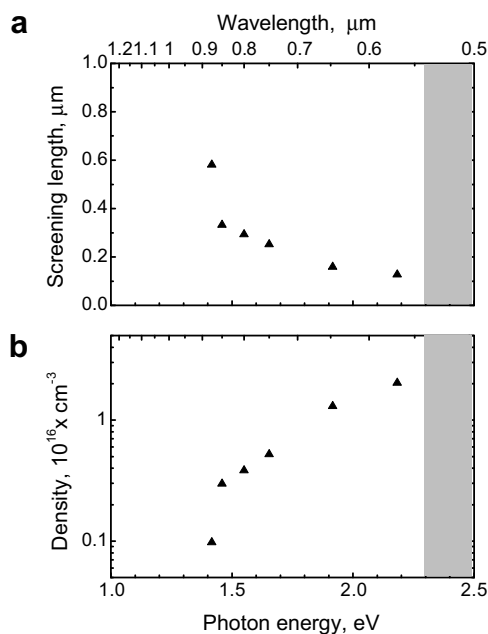


Fig. 3. Spectral dependences of (a) Debye screening length and (b) effective trap density. With gray color is shown the range of band-to-band absorption.

The beam coupling observed in SPS:Pb appeared to be strongly intensity dependent. The grating spacing dependences of the gain factor measured experimentally at $\lambda = 0.647 \mu\text{m}$ for different intensities are shown in Fig. 4a; the solid lines represent fits of Eq. (2) to the experimental data. The intensity dependence of the largest gain factor extracted from above data is shown in Fig. 4b. In photorefractive crystals, the gain factor is usually intensity dependent only within the intensity range where the photorefractive nonlinearity is not yet saturated, i.e., where the photoconductivity $\sigma_{\text{ph}} = \kappa I$ is comparable or smaller than the dark conductivity σ_d (see the second factor in Eq. (2)). In $\text{Sn}_2\text{P}_2\text{S}_6$ one more origin was revealed for the intensity dependence of Γ [12]: the Debye screening length ℓ_s (that enters the third factor in Eq. (2)) appeared to be intensity dependent, too.

The fits of the data presented in Fig. 4a show that the largest gain factor is achieved at different fringe spacing for different light intensities, as it is plotted in Fig. 5a. This clearly points to the intensity dependence of the screening length. The absolute changes of ℓ_s are not too large, no more than 20%. They result, however, from more important changes of the effective trap density. Fig. 5b represents the relevant intensity dependence of N_{eff} calculated with Eq. (3). Thus, we can conclude that similar to the nominally undoped SPS in Pb-doped material there are two reasons for the intensity dependence of the gain factor. Note also that the absolute values of the effective trap density in SPS:Pb is larger than in nominally undoped material what proves the efficiency of the selected dopant. The lar-

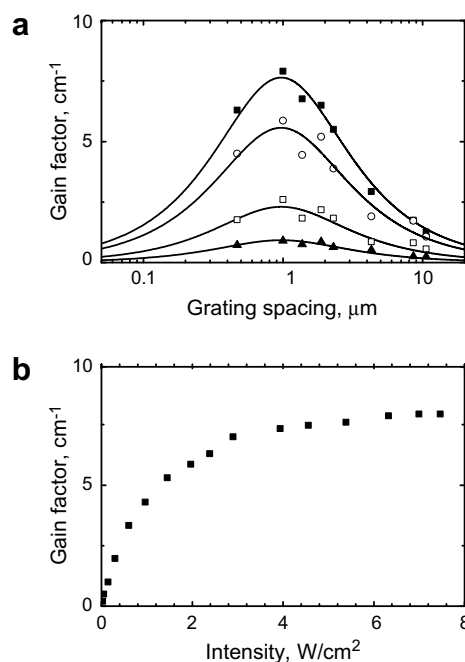


Fig. 4. (a) Gain factor versus grating spacing for different light intensities, 0.15 W/cm^2 (triangles), 0.5 W/cm^2 (open squares), 2.5 W/cm^2 (dots), and 10 W/cm^2 (filled squares). Solid lines show the fit of Eq. (2) to the data. (b) Intensity dependence of the largest gain factor.

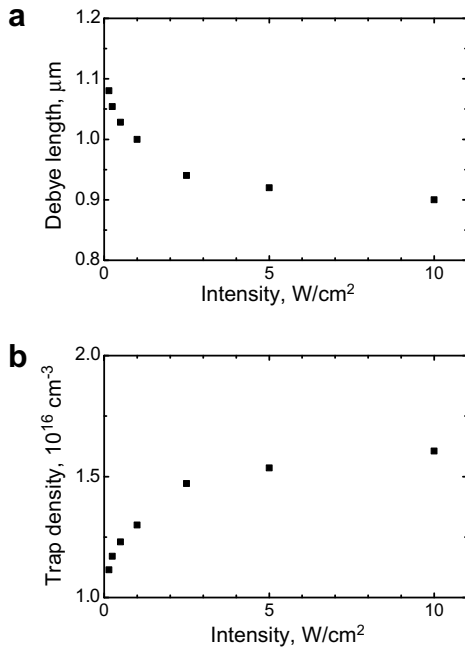


Fig. 5. Intensity dependence of (a) Debye screening length and (b) effective trap density.

ger effective trap density should soften the space charge limitations and should result, in particular, in an improvement of the gain factor for coupling of counterpropagating waves [13] providing that the samples are perfectly poled.

The temporal dynamics of the beam coupling was also the topic of our study. From the build-up of the output signal intensity shown in Fig. 1 the characteristic time τ of the space-charge grating can be extracted which depends on the dielectric relaxation time, the grating spacing and the characteristic transport lengths [9]

$$\frac{1}{\tau} = \frac{\sigma_d + \kappa I}{\epsilon \epsilon_0} \cdot \frac{1 + K^2 \ell_s^2}{1 + K^2 \ell_D^2} \quad (4)$$

Here $\ell_D = \sqrt{\frac{k_B T}{e} \mu \tau_c}$ is the diffusion length, μ is the carrier mobility, and τ_c is the carrier lifetime.

The value of I_{sat} can be found from the fit of Eq. (2) to experimental data of Fig. 4b. This fit takes into account the intensity variation of ℓ_s that are extracted from the data of Fig. 4a.

At first, the intensity dependence of the reciprocal decay time $1/\tau$ was measured for recording of a grating with $\Lambda = 1 \mu\text{m}$ at $\lambda = 0.647 \mu\text{m}$ (Fig. 6). The linear dependence shows the fit of Eq. (4) to the experimental data. Taking into account that for the conditions $K^2 \ell_s^2 < 1$ it is possible to extract from this fit the so-called saturation intensity, i.e., the intensity at which the photoconductivity equals the dark conductivity, $I_{\text{sat}} = \sigma_d/\kappa$. The value of I_{sat} can be found easily also from the extrapolation of the linear dependence to $1/\tau = 0$. For our particular SPS:Pb sample the fit reveals 1.5 W/cm^2 what is quite close to $\approx 1 \text{ W/cm}^2$, evaluated from Fig. 4b. The slight difference can be

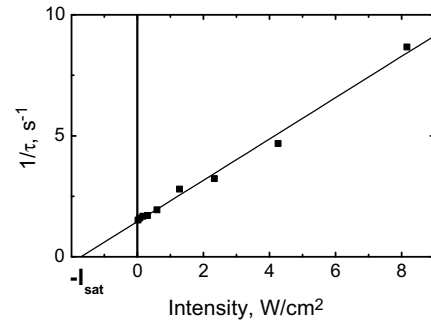


Fig. 6. Reciprocal relaxation time versus light intensity for a grating with $\Lambda = 1 \mu\text{m}$ at $\lambda = 0.647 \mu\text{m}$. Solid line shows fit of Eq. (4) to the measured data. Extrapolation of straight line to $1/\tau = 0$ gives a value of saturation intensity $I_{\text{sat}} = \sigma_d/\kappa$.

attributed to the intensity dependence of N_{eff} that is especially important just below $I = 3 \text{ W/cm}^2$.

To extract more information from the dynamics of space charge build-up it is useful to plot the reciprocal time normalized to the light intensity ($1/\tau I$) as a function of the squared spatial frequency K^2 (Fig. 7) for the intensities $I \gg I_{\text{sat}}$ and wavelength $0.568 \mu\text{m}$. As it was mentioned above for small values of K^2 the correction factor in Eq. (4) that depends on characteristic transport lengths is vanishing, and the decay time becomes identical to the dielectric relaxation time. Thus, the specific photoconductivity normalized to the dielectric constant can be evaluated, $\kappa/\epsilon \epsilon_0 \approx 1000 \text{ cm}^2/\text{Ws}$. For the other limiting case of very large K^2 the ratio of transport lengths can be evaluated, $(\ell_D/\ell_s) = 7.8/0.8 \approx 10$. With the Debye screening length known from previous experiment, $\ell_s = 0.13 \mu\text{m}$, the diffusion length can be evaluated $\ell_D = 1.3 \mu\text{m}$, and the carrier lifetime-mobility product is estimated to be $\mu \tau_c = 65 \mu\text{m}^2/\text{V}$.

Similar measurements have been performed at other light wavelengths. Fig. 8a, b represent the relevant spectral dependences for approximately 4 W/cm^2 intensity at any particular wavelength. These graphs show unambiguously the qualitative tendency: the characteristic decay time of photorefraction grows-up with increasing wavelength while the gain factor drops down.

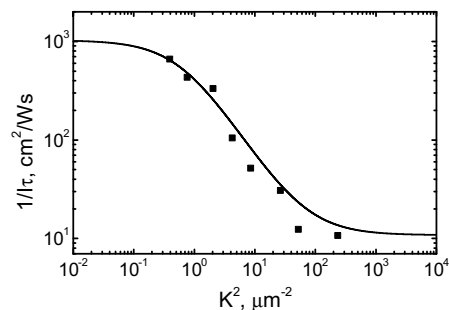


Fig. 7. Reciprocal relaxation time normalized to the light intensity versus squared spatial frequency of the photorefractive grating measured at $I \gg I_{\text{sat}}$. Solid line shows a fit of Eq. (4) to the data within the limit $\kappa I \gg \sigma_d$.

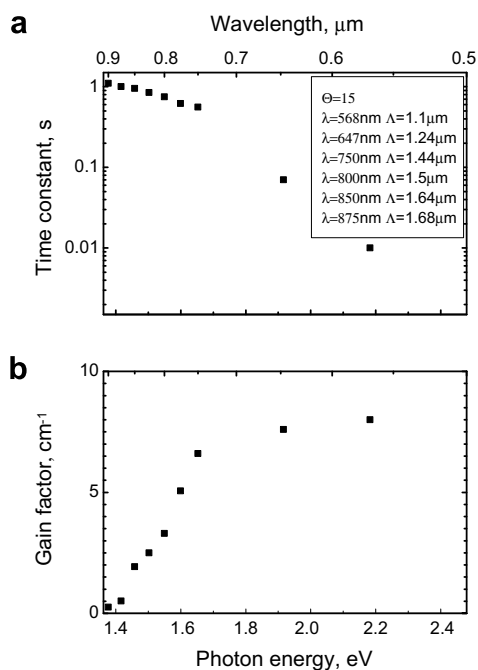


Fig. 8. Spectra of (a) photorefractive decay time and (b) beam coupling gain factor.

4. Conclusions

The photorefractive properties of Pb-doped $\text{Sn}_2\text{P}_2\text{S}_6$ are studied within the wavelength range from the forbidden band gap up to the sensitivity edge at $0.9 \mu\text{m}$. This material shows several advantages as compared with nominally undoped $\text{Sn}_2\text{P}_2\text{S}_6$: (i) it features the increased effective trap density and smaller Debye screening length, (ii) no decrease of the beam coupling is observed in the steady-state indicating that the compensation grating does not show up, (iii) the preliminary sensitization via pre-exposure to white light is not needed for getting the gain factor up to

10 cm^{-1} . This improvement is achieved, however, within a more narrow range of the spectral sensitivity which does not go beyond $0.9 \mu\text{m}$.

Acknowledgements

Financial support of the Deutsche Forschungsgemeinschaft (GRK695, IM37/2-2, TFB13-04) is gratefully acknowledged. The authors are grateful to E. Krätzig and S. Odoulov for helpful discussion.

References

- [1] M. Jazbinsek, A. Grabar, I. Stoyka, A. Shumelyuk, G. Montemezzani, P. Günter, in: P. Gunter, J.-P. Huignard (Eds.), *Photorefractive Materials and their Applications*, vol.2, Springer, 2007, pp. 327–362.
- [2] M. Weber, F. Rickermann, G. von Bally, A. Shumelyuk, S. Odoulov, *Optik* 111 (2000) 333.
- [3] S. Odoulov, A. Shumelyuk, U. Hellwig, R. Rupp, A. Grabar, I. Stoyka, *J. Opt. Soc. Am. B* 13 (1996) 2352.
- [4] A. Shumelyuk, S. Odoulov, Yi. Hu, E. Krätzig, G. Brost, CLEO'98 Technical Digest, Optical Society of America, 1998, p. 171.
- [5] T. Bach, M. Jazbinsek, G. Montemezzani, P. Günter, A. Grabar, I. Stoika, Yu. Vysochanskii, *J. Opt. Soc. Am. B* 24 (2007) 1535.
- [6] M. Jazbinsek, G. Montemezzani, P. Günter, A. Grabar, I. Stoika, Yu. Vysochanskii, *J. Opt. Soc. Am. B* 20 (2003) 1241.
- [7] A. Shumelyuk, S. Odoulov, D. Kip, E. Krätzig, *Appl. Phys. B* 72 (2001) 707.
- [8] D. Haertle, G. Caimi, A. Haldi, G. Montemezzani, A.A. Grabar, I. Stoyka, Yu.M. Vysochanski, *Opt. Commun.* 215 (2002) 333.
- [9] L. Solymar, D.J. Webb, A. Grunnet-Jepsen, *The Physics and Applications of Photo-refractive Materials*, Clarendon press, Oxford, 1996.
- [10] B. Sturman, P. Mathey, H.R. Jauslin, S. Odoulov, A. Shumelyuk, *J. Opt. Soc. Am. B* 24 (2007) 1303.
- [11] J. Seres, S. Stepanov, S. Mansurova, A. Grabar, *J. Opt. Soc. Am. B* 17 (2000) 1986.
- [12] A. Shumelyuk, CLEO'01 Technical Digest, Optical Society of America, 2001, p. 469.
- [13] M. Weber, G. von Bally, A. Shumelyuk, S. Odoulov, *Appl. Phys. B* 68 (1999) 959.